Genotyping

All polymerase chain reactions were carried out in a PTC-200 DNA Engine thermocycler (MJ Research) in 10-μl reactions containing 0.5 μM of each primer, 5 ng DNA, 0.25 mM dNTPs (Pharmacia), 1.5 mM $MgCl_2$, and 0.25 units Taq polymerase (PE Applied Biosystems). The cycling conditions for all primer pairs were 1 cycle of 95 °C for 1 min 45 s, 56 °C for 45 s and 72 °C for 45 s; 5 cycles of 94 °C for 45 s, 56 °C for 45 s and 72 °C for 45 s; and 30 cycles of 90 °C for 45 s, 56 °C for 45 s and 72 °C for 45 s, followed by a final cycle of 72 °C for 5 min. PCR products from 3 to 6 different primer pairs were then pooled and analysed on a 96-lane gel on an ABI377 with Gene Scan 2.1 software (Applied Biosystems) and GENESCAN-500 TAMRA (Applied Biosystems) used as internal size standard.

Linkage map construction

A genetic linkage map was created using JoinMap version 2.0 (ref. 10) on a locus file containing genotypes of 227 microsatellite loci in 92 backcross progeny, with the population type set for segregation of up to four alleles per locus (cross-pollinator). The JMGRP module of JoinMap was used with a LOD score threshold of 4.0 to assign 219 of the 227 loci to 26 linkage groups. The JMREC module was then used on each of the linkage groups to determine phase information for each locus. For each linkage group, a map was created with the JMMAP module: Kosambi mapping function, LOD threshold of 0.001, recombination threshold of 0.499, jump threshold of 5.0, triplet value of 5.0, and no fixed order. A ripple was performed after all markers on the linkage group were added to the map.

Morphological analysis

Fish were fixed in 10% buffered formalin for at least 1 week, placed in distilled H_2O (dH_2O) for 24 h, stained with 0.008% alizarin red in 1% KOH for 24 h, placed in dH_2O for 24 h, and placed in 37% isopropyl alcohol for final storage. Measurements were done with Vernier callipers accurate to 0.02 mm. Lateral plates were counted on both sides of the body, and the number of long and short gill rakers were counted on the left side of the first gill arch.

QTL mapping

All morphological traits were analysed with MapQTL 3.0 (ref. 28) using the interval mapping method which fits a single QTL model that is based on four possible segregating genotypes and does not assume a particular model of relationship between benthic and limnetic alleles. The parameters used were: mapping step size of 5.0, maximum of 200 iterations, and functional tolerance value of $1.0e^{-8}$. A maximum of five flanking markers were used to resolve incomplete genotypes. Significance thresholds for linkage were chosen using conservative criteria for genome-wide linkage mapping in non-inbred individuals: suggestive linkage of LOD $\geq$ 3.2, significant linkage of LOD $\geq$ 4.5 (ref. 29). Significance thresholds were confirmed by permutation tests in MapQTL 4.0, with a genome-wide significance level of $\alpha = 0.05$, $n = 1{,}000$ for significant linkages and a chromosome-wide significance level of $\alpha = 0.05$, $n = 1{,}000$ for suggestive linkages. Suggestive loci were only reported for those traits which were also influenced by one or more significant QTL. Multiple QTL model (MQM) mapping with initial QTL did not change the results. Calculation of the percentage of phenotypic variance explained by a QTL was done in MapQTL 3.0 on the basis of the population variance found within the progeny of the cross.

Received 22 June; accepted 7 November 2001.

1. Bell, M. A. & Foster, S. A. *The Evolutionary Biology of the Threespine Stickleback* (Oxford Science, New York, 1994).
2. McPhail, J. D. in *The Evolutionary Biology of the Threespine Stickleback* (eds Bell, M. A. & Foster, S. A.) 399–437 (Oxford Univ. Press, New York, 1994).
3. Ridgway, M. S. & McPhail, J. D. Ecology and evolution of sympatric sticklebacks (*Gasterosteus*): mate choice and reproductive isolation in the Enos Lake species pair. *Can. J. Zool.* **62,** 1813–1818 (1984).
4. Nagel, L. & Schluter, D. Body size, natural selection, and speciation in sticklebacks. *Evolution* **52,** 209–218 (1998).
5. Hatfield, T. & Schluter, D. Ecological speciation in sticklebacks: environment-dependent hybrid fitness. *Evolution* **53,** 866–873 (1999).
6. Vamosi, S. M. & Schluter, D. Sexual selection against hybrids between sympatric stickleback species: evidence from a field experiment. *Evolution* **53,** 874–879 (1999).
7. Rico, C., Zadworny, D., Kuhnlein, U. & Fitzgerald, G. J. Characterization of hypervariable microsatellite loci in the threespine stickleback *Gasterosteus aculeatus*. *Mol. Ecol.* **7,** 271–272 (1993).
8. Taylor, E. B. Microsatellites isolated from the threespine stickleback *Gasterosteus aculeatus*. *Mol. Ecol.* **7,** 925–931 (1998).
9. Largiader, C. R., Fries, V., Kobler, B. & Bakker, C. M. Isolation and characterization of microsatellite loci from the three-spined stickleback (*Gasterosteus aculeatus* L.). *Mol. Ecol.* **8,** 342–344 (1999).
10. Stam, P. & Van Ooijen. JoinMap, version 2.0: Software for the calculation of genetic linkage maps. (Centre for Plant Breeding and Reproduction Research, Wageningen, 1995).
11. Chen, T.-R. & Reisman, H. M. A comparative study of the North American species of sticklebacks (Teleostei: Gasterosteidae). *Cytogenetics* **9,** 321–332 (1970).
12. Bentzen, P. & McPhail, J. D. Ecology and evolution of sympatric sticklebacks (*Gasterosteus*): specialization for alternative trophic niches in the Enos Lake species pair. *Can. J. Zool.* **62,** 2280–2286 (1984).
13. Schluter, D. Adaptive radiation in sticklebacks: size, shape, and habitat use efficiency. *Ecology* **74,** 699–709 (1993).
14. Hatfield, T. Genetic divergence in adaptive characters between sympatric species of stickleback. *Am. Nat.* **149,** 1009–1029 (1997).
15. Hagen, D. W. & Gilbertson, L. G. Geographic variation and environmental selection in *Gasterosteus aculeatus* L. in the Pacific Northwest, America. *Evolution* **26,** 32–51 (1972).
16. Moodie, G. E. E. Predation, natural selection and adaptation in an unusual threespine stickleback. *Heredity* **28,** 155–167 (1972).
17. Reimchen, T. E. Spine deficiency and polymorphism in a population of (*Gasterosteus aculeatus*): an adaptation to predators? *Can. J. Zool.* **58,** 1232–1244 (1980).
18. Reimchen, T. E. Structural relationship between spines and lateral plates in threespine stickleback (*Gasterosteus aculeatus*). *Evolution* **37,** 931–946 (1983).
19. Hawthorne, D. J. & Via, S. Genetic linkage of ecological specialization and reproductive isolation in pea aphids. *Nature* **412,** 904–907 (2001).
20. Lynch, M. & Walsh, J. B. *Genetics and Analysis of Quantitative Traits* (Sinauer, Massachusetts, 1998).
21. Ahn, D. & Gibson, G. Axial variation in the threespine stickleback: genetic and environmental factors. *Evol. Dev.* **1,** 100–112 (1999).
22. Reimchen, T. E. Predator-induced cyclical changes in lateral plate frequencies of *Gasterosteus*. *Behavior* **132,** 1079–1094 (1995).
23. Swain, D. P. Selective predation for vertebral phenotype in *Gasterosteus aculeatus*: reversal in the direction of selection at different larval sizes. *Evolution* **46,** 998–1013 (1992).
24. Orr, H. A. The genetics of species differences. *Trends Ecol. Evol.* **16,** 343–350 (2001).
25. Beavis, W. D. in *Molecular Dissection of Complex Traits* (ed. Paterson, A. H.) 145–162 (CRC Press, Boca Raton, 1998).
26. Hinegardner, R. Evolution of cellular DNA content in teleost fishes. *Am. Nat.* **102,** 517–523 (1968).
27. Rozen, S. & Skaletsky, H. J. Primer3; code available at http://www-genome.wi.mit.edu/genome_software/other/primer3.html (1997).
28. VanOoijen, J. W. & Maliepard, C. MapQTL, version 3.0: Software for the calculation of QTL positions on genetic maps. (Centre for Plant Breeding and Reproduction Research, Wageningen, 1996).
29. VanOoijen, J. W. LOD significance thresholds for QTL analysis in experimental populations of diploid species. *Heredity* **83,** 613–624 (1999).
30. Bell, M. A. in *Evolutionary Genetics of Fishes* (ed. Turner, B. J.) 431–528 (Plenum, New York, 1984).

Supplementary Information accompanies the paper on *Nature*'s website (http://www.nature.com).

Acknowledgements

We thank S. Anderson, R. Melzer, K. Tsui, C. Uhlick and R. Vega for technical assistance. D.S. was supported by a Natural Sciences and Engineering Research Council of Canada research grant. C.L.P. is a research associate and D.M.K. is an assistant investigator of the Howard Hughes Medical Institute.

Competing interests statement

The authors declare that they have no competing financial interests.

Correspondence and requests for materials should be addressed to D.M.K. (e-mail: kingsley@cmgm.stanford.edu). GenBank accession numbers for stickleback microsatellite markers are G72126–G72334.

Dynamic properties of neurons in cortical area MT in alert and anaesthetized macaque monkeys

Christopher C. Pack, Vladimir K. Berezovskii & Richard T. Born

Department of Neurobiology, Harvard Medical School, 220 Longwood Avenue, Boston, Massachusetts 02115, USA

In order to see the world with high spatial acuity, an animal must sample the visual image with many detectors that restrict their analyses to extremely small regions of space. The visual cortex must then integrate the information from these localized receptive fields to obtain a more global picture of the surrounding environment. We studied this process in single neurons within the middle temporal visual area (MT) of macaques using stimuli that produced conflicting local and global information about stimulus motion. Neuronal responses in alert animals initially reflected predominantly the ambiguous local motion features, but gradually converged to an unambiguous global representation. When the same animals were anaesthetized, the integration of local motion signals was markedly impaired even though neuronal responses remained vigorous and directional tuning characteristics were intact. Our results suggest that anaesthesia preferentially

© 2001 Macmillan Magazines Ltd

affects the visual processing responsible for integrating local signals into a global visual representation.

Figure 1a shows an example of the 'aperture problem'[1,2]: a moving edge viewed through a small aperture only provides information about the component of motion perpendicular to its orientation. In the primate visual system, the small receptive fields of neurons at stages up to and including the primary visual cortex (V1) function as apertures, and so are faced with this problem. Therefore, neurons in extrastriate cortex must integrate motion information in such a way as to correct for systematic errors in their inputs. In order to examine this process, we have recorded the responses of neurons in area MT—an important motion-processing region in extrastriate cortex—to stimuli designed to generate locally ambiguous motion measurements in V1 cells.

Figure 2a shows the response of a typical MT neuron in an alert monkey to the grating stimulus shown in Fig. 1a (see Methods for experimental details). The neuron responds strongly to motion to the left (its preferred direction), but weakly to other motion directions, and negligibly to rightward motion. Based on this tuning curve, we can make two different predictions about this neuron's response to the plaid stimulus in Fig. 1b. If the orientations of the component gratings of the plaid are significantly different, then when one grating moves to the left, the second grating will move in a direction that by itself generates no response. To the extent that the neuron 'sees' only the local motion cues generated by each grating, the tuning curve for the plaid stimulus should have a separate peak for each direction of plaid motion that moves one of the gratings leftward. The difference in these peaks should be close to the difference in the orientations of the gratings. This has been termed the 'component' prediction[3]. Alternatively, if the neuron integrates the global motion of the plaid stimulus, then the response should be strongest when the entire pattern moves leftward. This is the 'pattern' prediction[3].

We tested this neuron with plaid stimuli consisting of two gratings that differed in their orientations by 144°. Figure 2b shows the earliest directionally selective response, which occurred at a latency of 62 ms. The direction tuning is clearly bimodal, consistent with the component prediction. However, the subsequent direction tuning, determined by averaging over the last 1,500 ms of stimulus presentation, is unimodal and peaks for leftward plaid motion (Fig. 2c), consistent with the pattern prediction. This indicates that the neural responses ultimately reflected the computation of plaid pattern motion from the component gratings.

We note that human perception of the stimuli used in these experiments usually conforms to the pattern prediction[4,5], but the inputs from monkey V1 cells always conform to the component prediction[3,6]. In this regard, we can say that the computation of pattern motion in MT is more closely correlated with normal perception. A simple way to test this idea is to repeat the experiment in the anaesthetized animal.

Figure 2d–f shows data from a different neuron recorded from approximately the same part of MT while the same animal was anaesthetized with isoflurane (see Methods for details). This neuron failed to compute the direction of plaid motion, responding instead to the plaid components for the duration of the stimulus presentation. We recorded 42 MT neurons in the anaesthetized animals (with monocular viewing), and 35 MT neurons while the same two animals were awake and fixating binocularly. We analysed the responses by computing the correlations[3] between the observed

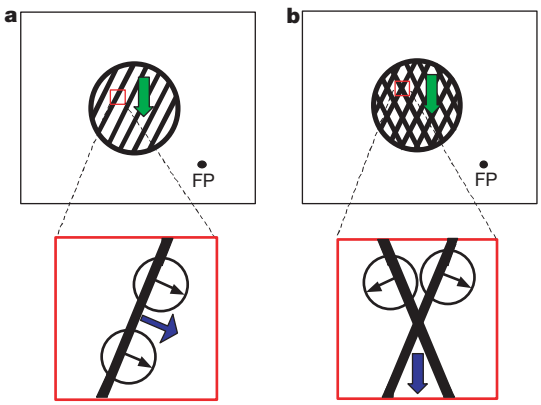

Figure 1 Experimental stimuli. Green arrows represent the actual direction of stimulus motion; black arrows, local motion cues; blue arrows, the perceived direction for human observers. Large circles in the top row depict an MT receptive field. **a**, A grating stimulus consisting of alternating black and white bars, the endpoints of which are not visible. **b**, A plaid stimulus constructed by superimposing two gratings. Because of the aperture problem, motion of the entire plaid pattern generates differing local motion cues (black arrows) that, if combined properly, yield the actual direction of plaid motion (blue arrow). Stimulus contrast has been reversed here for clarity. FP, fixation point.

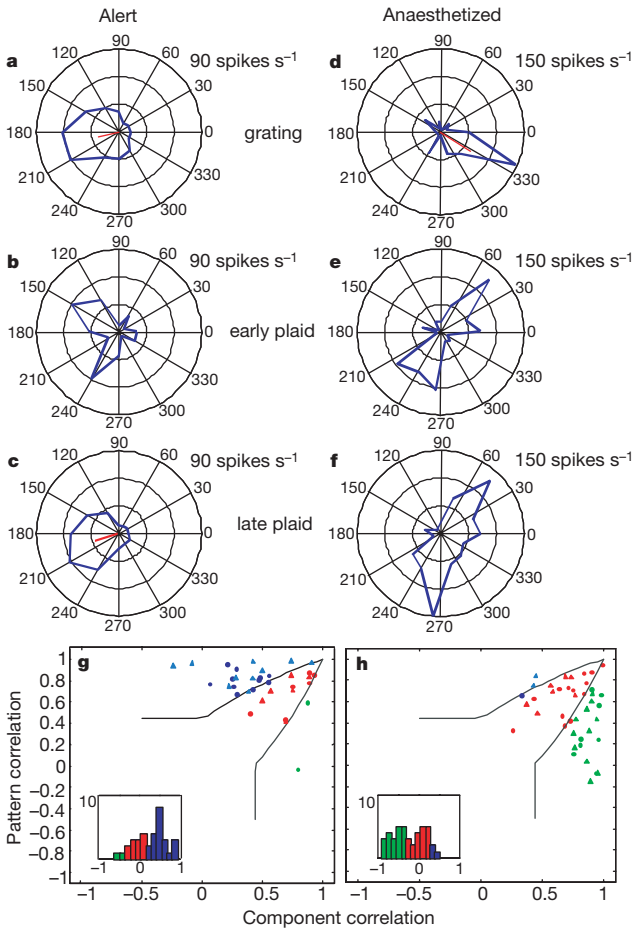

Figure 2 Results for plaid stimuli. **a**, Responses to grating motion for an MT cell recorded in an alert animal. Direction tuning is represented in polar coordinates, with the angle representing the grating direction and the radius representing the response in spikes per second. The red line indicates the vector average of the responses to each direction. **b**, Direction tuning of the first 20 ms of the cell's response to the plaid. **c**, Response of the same cell, averaged over the last 1,500 ms of stimulation. **d**–**f**, As for **a**–**c**, but in a different cell while the animal was anaesthetized. **g**, Classification of cells from alert animals according to correlations with the component and pattern predictions. Points upward and leftward from the black lines were classified as pattern cells (blue). Points downward and rightward from the black lines were classified as component cells (green). Points between the lines were poorly correlated with both predictions (red). The different symbols (triangle, circle) represent different monkeys. The histogram groups cells according to the strength of the pattern prediction. **h**, As for **g**, but cells recorded in anaesthetized animals.

© 2001 Macmillan Magazines Ltd

plaid responses and the two predictions described above (component and pattern; see Methods). The results are shown in Fig. 2g and h. In the alert animals, 60% of the neurons were classified as pattern cells, compared with only 6% classified as pure component cells, based on the difference in the correlation coefficients. When the animals were anaesthetized, 7% were classified as pattern cells and 45% as component cells. This was not related to effects of anaesthesia on basic neuronal response properties, such as direction selectivity, nor to differences related to monocular versus binocular viewing (see below). A comparison of the tuning bandwidths for grating stimuli showed that the populations were not significantly different (anaesthetized mean 83.3°, alert mean 90.3°; two-tailed t-test $P > 0.5573$), as has been shown previously for tuning curves in V1 (ref. 7) and MT[8].

By subtracting the variance accounted for by the pattern prediction from that accounted for by the component prediction, we obtained a pattern index[9], which describes the strength of the pattern prediction relative to the component prediction (see Methods). Positive values indicate close conformity with the pattern prediction, while negative values support the component prediction. Histograms of these values are shown in the lower left of Fig. 2g and h. A comparison of the pattern indices between the anaesthetized and alert populations indicates that these differences were highly significant (one-tailed t-test, $P < 0.0001$). Figure 3 shows that the shift from component responses to pattern responses in the alert animals (as in Fig. 2b, c) was typical of the MT population. The pattern index shifts from being strongly negative to strongly positive over a period of approximately 100 ms. This shift does not occur in the anaesthetized MT population. The same cells, when tested with tilted bar stimuli (as in ref. 10), responded primarily to the component of motion perpendicular to the orientation of the bars.

In order to ensure that these results were not due to differences between the two preparations (anaesthetized and alert) that were unrelated to anaesthesia, we conducted control experiments to test other potential confounding factors. Specifically, viewing was binocular in the alert case, but one eye was occluded in the anaesthetized experiments. Also, although the monkeys' vision was artificially corrected in the anaesthetized experiments (see Methods), some residual blurring may have occurred. To determine if these differences could explain our findings, we recorded from 10 additional neurons in an alert animal. For each neuron, three conditions were tested: binocular viewing, monocular viewing (one eye occluded), and monocular viewing with image blurred. The latter condition involved occluding one eye and defocusing the image by placing a +2-dioptre trial lens over the other eye. Of the 10 cells recorded, 5 were classified as pattern cells, and neither the monocular viewing nor the blurring caused any of these to switch to a component classification. The mean pattern indices in the binocular, monocular and blurred conditions were 0.20, 0.24 and 0.25. Pairwise comparisons of the component and pattern correlations across the different viewing conditions revealed no significant changes (two-tailed t-test following Fisher's z-transform, $P > 0.19$ in all cases). We conclude that it is extremely unlikely that these viewing differences were responsible for the differences in motion integration shown in Fig. 2.

Our results suggest that the process of resolving ambiguous local information into a global representation is significantly impaired by general anaesthesia. This explanation connects our recent findings in alert animals[10] with previous neurophysiological studies in anaesthetized animals, which indicate that a minority of cells encode pattern motion[3,11,12]. We also found that pattern motion is computed accurately by a minority of MT cells (7%) under anaesthesia, but that in alert animals this percentage increases greatly (60%). It should be noted that the percentage of MT pattern cells found in previous studies of anaesthetized animals[11,12] has been closer to 25%, which is somewhat higher than what we found. This may be due to stimulus differences. For instance, our grating stimuli were separated by a larger orientation difference, and had a lower spatial frequency, than the gratings used in previous studies[3,9]. The low spatial frequency was chosen to reduce the number of grating intersections, which increase in number with increasing spatial frequency[13], and provide an unambiguous cue as to the actual pattern direction.

Computational models of motion integration generally consist of two or more stages. The first stage, usually assigned to V1, contains units that extract the component of motion perpendicular to the orientation of contours[5]. That is, they are limited by the aperture problem. Our finding that directional responses to grating stimuli are not impaired by anaesthesia suggests that this stage is largely intact in the anaesthetized animals. The second stage of motion processing, thought to correspond to MT, is responsible for integrating motion signals in such a way as to overcome the biases introduced in the first stage. It has been shown that this can be accomplished by an appropriate feedforward weighting of V1 inputs[14]. However, some elaboration of the feedforward model would be necessary to account for our observations on the temporal dynamics of motion integration.

One possible elaboration is that MT neurons receive information about the motion of features such as grating intersections via an intermediate 'non-Fourier' stage, requiring a slightly longer latency[15]. If this model is correct, our results suggest a selective

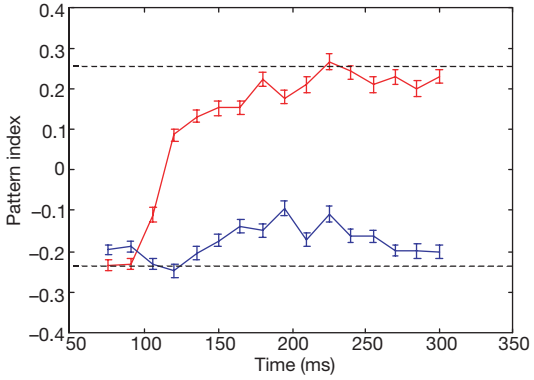

Figure 3 Change in the pattern index over time. Figure shows the mean pattern index for the populations of MT cells recorded from alert animals (red) and anaesthetized animals (blue). The horizontal dotted black lines indicate the mean value of the time-averaged pattern index for the alert population (upper line) and anaesthetized population (lower line). Data are grouped in 15-ms bins. Error bars indicate standard error of the mean.

© 2001 Macmillan Magazines Ltd

impairment of the intermediate stage. Such an effect might also explain the finding that MT neurons more accurately encode the direction of non-Fourier motion stimuli in alert animals[16] than in anaesthetized animals[17]. Second, and more generally, anaesthesia could act on an early stage, by disrupting the temporal properties of neurons in the thalamus[18]. A third possibility is that the delayed response to the global properties of the stimulus, and its suppression by anaesthesia, are signatures of cortical feedback, as has been suggested by studies of contextual modulation in V1 (refs 19–21). Feedback could be useful for sharpening the tuning generated by feedforward inputs[15] or for propagating unambiguous motion signals to ambiguous regions of the visual representation[22,23]. Such mechanisms should be identifiable by manipulations such as cortical cooling, which have proven useful in the studies of functional connectivity in other parts of the visual system[24]. □

Methods

Visual stimuli and recordings from alert monkeys

Recordings were obtained from single units in alert monkeys, as described previously[25]. Each animal underwent a magnetic resonance imaging (MRI) scan to locate MT within the coordinates of a plastic grid inserted in the recording cylinder. The same grid, along with a guide tube, was used to guide insertion of the microelectrode. MT was identified on the basis of depth, prevalence of direction-selective neurons, receptive field size, and visual topography. Visual stimuli consisted of gratings and plaids, and were viewed binocularly at a distance of 57 cm. The gratings were square-wave, 0.5 cycles per degree with a duty cycle of 0.4. Plaids were constructed by overlapping two gratings moving in directions separated by 144°. There were no luminance differences at the intersections of the gratings. The resulting motion was informally judged to be completely coherent by human observers. Plaid speed was always faster than grating speed, as dictated by stimulus geometry[5]. All stimuli were generated by a PC containing a video board (SGT-Plus, Number Nine Corp), and had a luminance of 13.9 cd m^{-2} against a dark background (0.025 cd m^{-2}). For each cell, each stimulus was presented 5 times in blockwise random order for 2 s. To separate directional responses from on-transients and orientation responses, each stimulus remained stationary for 240 ms before moving. For gratings and plaids, motion direction was generally sampled at 24° intervals, although a few cells were measured at 30° intervals. Neuronal signals were recorded extracellularly using tungsten microelectrodes (FHC) with standard amplification and filtering (BAK Electronics), while the monkeys fixated a small spot. Fixation was monitored with an eye coil[26] and required to be within 1° of the spot for the monkeys to obtain a liquid reward. Single units were isolated using a dual time and amplitude window discriminator (BAK).

Recordings from anaesthetized monkeys

We used the same two monkeys for alert experiments and for recordings under general anaesthesia (isoflurane), as previously described[27]. One monkey participated in two anaesthetized recording sessions, and the second monkey participated in one session. Alert recordings were obtained both before and after the anaesthetized recordings for both animals. To ensure proximity of the recording sites between the two preparations, electrodes were inserted into the same grid positions with the same guide tubes in the same recording chambers, restricting the variability in electrode position to 1 mm. This was confirmed by the nearly identical distributions of receptive field eccentricities in the alert and anaesthetized conditions (4°–18°). Anaesthesia was induced with ketamine (15 mg kg^{-1}, intramuscular). The animal was intubated, and anaesthesia was maintained with isoflurane (0.5–1% in oxygen). Electroencephalograms were not recorded. Throughout the experiment the electrocardiogram and end-tidal pCO_2 were continuously monitored, and any changes indicative of a lightening of anaesthesia were immediately corrected by increasing the level of isoflurane. The animal's head was immobilized in a stereotaxic frame using the same head post used in the alert experiments. The animal was paralysed with a continuous intravenous infusion of vecuronium bromide (0.05 mg kg^{-1} h^{-1}). Gas-permeable contact lenses of the appropriate basal curvature were placed over the eyes. A streak retinoscope was used to measure the refractive state, and trial lenses were used to bring the stimulus display monitor, at a distance of 57 cm, into focus. The location of the fovea was back-projected onto the display monitor using an ophthalmoscope fitted with a reversing prism. This was re-checked periodically throughout the experiment.

Optics

In the alert animals, stimuli were viewed binocularly, whereas viewing in the anaesthetized experiments was monocular. Both monkeys had clear ocular media and were refracted while under anaesthesia with accommodation paralysed (1% atropine sulphate) using streak retinoscopy performed by an experienced operator (R.T.B.). Monkey 1 had a small hyperopic error of +0.25 dioptres and monkey 2 had a slightly larger hyperopic error (+1.75 dioptres). These were corrected using trial lenses during experiments under anaesthesia. For alert experiments, the stimuli were presented on a monitor that was 57 cm from the animal. This would require, for monkey 2, +3.5 dioptres of accommodation, which is well within the range of the accommodative mechanism of the primate eye.

Data analysis

For each cell, component and pattern predictions were generated from grating responses using an extension[6] of the partial correlation measure[3]. Briefly, the component prediction is the sum of the observed grating responses rotated by 72° clockwise and anticlockwise. The pattern prediction is identical to the grating response. The pattern correlation is given by $R_p = (r_p - r_c r_{pc})/[(1 - r_c^2)(1 - r_{pc}^2)]^{1/2}$, where r_p is the raw correlation of the data with the pattern prediction, r_c is the raw correlation of the data with the component prediction, and r_{pc} is the correlation of the two predictions. The partial correlation coefficient for the component prediction, R_c, is obtained by exchanging r_c and r_p in the above equation. A measure of pattern selectivity relative to component selectivity is obtained by subtracting the variance accounted for by the component prediction from that accounted for by the pattern prediction. This pattern index is given by $(R_p^2 - R_c^2)$.

Received 30 August; accepted 31 October 2001.

1. Wallach, H. Uber visuell wahrgenommene Bewegungsrichtung. *Psychol. Forsch.* **20,** 325–380 (1935).
2. Marr, D. & Ullman, S. Directional selectivity and its use in early visual processing. *Proc. R. Soc. Lond. B* **211,** 151–180 (1981).
3. Movshon, J. A., Adelson, E. H., Gizzi, M. S. & Newsome, W. T. The analysis of moving visual patterns. *Exp. Brain Res. Suppl.* **11,** 117–151 (1986).
4. Stoner, G. R., Albright, T. D. & Ramachandran, V. S. Transparency and coherence in human motion perception. *Nature* **344,** 153–155 (1990).
5. Adelson, E. H. & Movshon, J. A. Phenomenal coherence of moving visual patterns. *Nature* **300,** 523–525 (1982).
6. Movshon, J. A. & Newsome, W. T. Visual response properties of striate cortical neurons projecting to area MT in macaque monkeys. *J. Neurosci.* **16,** 7733–7741 (1996).
7. Snodderly, D. M. & Gur, M. Organization of striate cortex of alert, trained monkeys (*Macaca fascicularis*): ongoing activity, stimulus selectivity, and widths of receptive field activating regions. *J. Neurophysiol.* **74,** 2100–2125 (1996).
8. Mikami, A., Newsome, W. T. & Wurtz, R. H. Motion selectivity in macaque visual cortex. II. Spatiotemporal range of directional interactions in MT and V1. *J. Neurophysiol.* **55,** 1328–1339 (1986).
9. Stoner, G. R. & Albright, T. D. Neural correlates of perceptual motion coherence. *Nature* **358,** 412–414 (1992).
10. Pack, C. C. & Born, R. T. Temporal dynamics of a neural solution to the aperture problem in visual area MT of macaque brain. *Nature* **409,** 1040–1042 (2001).
11. Rodman, H. R. & Albright, T. D. Single-unit analysis of pattern-motion selective properties in the middle temporal visual area (MT). *Exp. Brain Res.* **75,** 53–64 (1989).
12. Castel-Branco, M., Goebel, R., Neuenschwander, S. & Singer, W. Neural synchrony correlates with surface segregation rules. *Nature* **405,** 685–689 (2000).
13. Alais, D., Wenderoth, P. & Burke, D. The size and number of plaid blobs mediate the misperception of type-II plaid direction. *Vision Res.* **37,** 143–150 (1997).
14. Simoncelli, E. P. & Heeger, D. J. A model of neuronal responses in visual area MT. *Vision Res.* **38,** 743–761 (1998).
15. Wilson, H. R., Ferrera, V. P. & Yo, C. A psychophysically motivated model for two-dimensional motion perception. *Vis. Neurosci.* **9,** 79–97 (1992).
16. Albright, T. D. Form-cue invariant motion processing in primate visual cortex. *Science* **255,** 1141–1143 (1992).
17. O'Keefe, L. P. & Movshon, J. A. Processing of first- and second-order motion signals by neurons in area MT of the macaque monkey. *Vis. Neurosci.* **15,** 305–317 (1998).
18. Mukherjee, P. & Kaplan, E. Dynamics of neurons in the cat lateral geniculate nucleus: in vivo electrophysiology and computational modeling. *J. Neurophysiol.* **74,** 1222–1243 (1995).
19. Lamme, V. A. The neurophysiology of figure-ground segregation in primary visual cortex. *J. Neurosci.* **15,** 1605–1615 (1995).
20. Lamme, V. A., Zipser, K. & Spekreijse, H. Figure-ground activity in primary visual cortex is suppressed by anesthesia. *Proc. Natl Acad. Sci. USA* **95,** 3263–3268 (1998).
21. Lamme, V. A. & Roelfsema, P. R. The distinct modes of vision offered by feedforward and recurrent processing. *Trends Neurosci.* **23,** 571–579 (2000).
22. Hildreth, E. C. *The Measurement of Visual Motion* (MIT Press, Cambridge, Massachusetts, 1984).
23. Lidèn, L. H. & Pack, C. C. The role of terminators and occlusion cues in motion integration and segmentation: A neural network model. *Vision Res.* **39,** 3301–3320 (1999).
24. Ferster, D., Chung, S. & Wheat, H. Orientation selectivity of thalamic input to simple cells of cat visual cortex. *Nature* **380,** 249–252 (1996).
25. Born, R. T., Groh, J. M., Zhao, R. & Lukasewycz, S. J. Segregation of object and background motion in visual area MT: effects of microstimulation on eye movements. *Neuron* **26,** 725–734 (2000).
26. Robinson, D. A method of measuring eye movement using a scleral search coil in a magnetic field. *IEEE Trans. Biomed. Eng.* **10,** 137–145 (1963).
27. Born, R. T. & Tootell, R. B. Spatial frequency tuning of single units in macaque supragranular striate cortex. *Proc. Natl Acad. Sci. USA* **88,** 7066–7070. (1991).

Acknowledgements

We thank P. Hendrickson for technical assistance, and M. Livingstone for comments on an earlier version of the manuscript. This work was supported by the NIH, The Whitehall Foundation and The Giovanni Armenise-Harvard Foundation for Scientific Research. C.C.P. was supported by a McDonnell-Pew fellowship.

Competing interests statement

The authors declare that they have no competing financial interests.

Correspondence and requests for materials should be addressed to C.C.P. (e-mail: cpack@hms.harvard.edu).

© 2001 Macmillan Magazines Ltd